

Effects of Time and Consolidation Method on Bond Strength between Fresh UHPC Layers

Megan Voss, Ph.D. (corresponding author) – Assistant Professor, University of Evansville, Evansville, IN, USA, Email: mv110@evansville.edu

Taylor Rawlinson, Ph.D. – Assistant Engineer, University of Florida, Gainesville, FL, USA, Email: taylor.rawlinson@essie.ufl.edu

Raid S. Alrashidi, Ph.D. – Graduate Research Assistant, University of Florida, Gainesville, FL, USA, Email: raid_saif@hotmail.com

Christopher Ferraro, Ph.D. – Assistant Professor, University of Florida, Gainesville, FL, USA, Email: ferraro@ce.ufl.edu

Trey Hamilton, Ph.D. – Professor Emeritus, University of Florida, Gainesville, FL, USA, Email: hrh@ufl.edu

Kyle Riding, Ph.D. – Professor, University of Florida, Gainesville, FL, USA, Email: kyle.riding@essie.ufl.edu

Abstract

Full-scale ultra-high performance concrete (UHPC) members often require multiple UHPC batches to meet the required volume. UHPC's "elephant skin" forms quickly and could lead to a weakened interface between the placements. This study investigated placement best practices for multiple UHPC batches to develop procedural specifications that reduce the prevalence of weak interfaces. UHPC mixes staggered in intervals of 10–35 minutes were placed in layers. The flow of the concrete mixes and the resistance of the elephant skin to penetration were measured. A set of three samples from each time interval was rodded, one was externally vibrated, and one was not consolidated (control). After curing, cores were drilled through both layers of concrete and pull-off tests were used to determine bond strength and failure location. Computerized Tomography (CT) scans of select samples were taken to understand how consolidation method affected fiber orientation at the layer interface. Results demonstrate that rodded specimens produced the fewest percentage of interface failures and the highest average strengths, but external vibration also reduced interface failures and increased strength at lower time intervals. CT results showed very few fibers crossing through the concrete interfaces, but rodded specimens had small regions of perpendicular fibers at the locations of rodding.

Keywords: bond, elephant skin, fiber orientation, interface strength, consolidation

1. Background

The exceptional strength and durability properties of UHPC make it an ideal material for many construction applications, but the properties of the material require different placement methods

in comparison to traditional concrete. For example, internal vibration used for normal concrete has been proven to increase fiber settlement and cause preferential fiber orientation in UHPC (CSA A23.1:19). Another unique quality of UHPC is the “elephant skin” that quickly forms on the concrete’s surface after it has been placed (Binard). This “elephant skin” is a rough crust that can form on the surface exposed to the ambient environment within minutes after casting (Yalçınkaya and Çopuroğlu). The combination of low water content and high amounts of superplasticizer results in early desiccation and stiffening of this skin. In addition to causing difficulties with surface finishing and trapped air, this elephant skin has the potential to cause a weak interface between concrete placed at different times or at different locations of a large specimen. The stiffness of the elephant skin on the first layer could prevent subsequent layers from intermixing and fibers from bridging the interface between the two layers. The Canadian UHPC guidelines recommend that in cases where the intersections of multiple UHPC wave fronts cannot be avoided, an “L” shaped rod or a propeller on a shaft should be inserted through the full depth of the concrete and twisted as it is pulled out (CSA A23.1:19), but it is not clear how much time must pass for wave fronts to be separate, and this method may be difficult in heavily-reinforced members.

The purpose of this research is to determine how the strength of the bond between two separate placements of UHPC changes with the amount of time between placements and varying concrete fresh properties. This is research especially applicable to precast concrete producers who make full-sized concrete specimens out of UHPC, which often require multiple concrete batches mixed from the same specialized UHPC mixer, allowing elephant skin to form and thicken. While significant research has been performed on the proper construction techniques for binding UHPC to hardened concrete or UHPC (Miguel A. Carbonell Muñoz et al.; Ganesh and Ramachandra Murthy; Graybeal), this research focuses on the best methods to ensure fresh UHPC binds well to UHPC that has stiffened after placement but not has yet reached initial set.

2. Materials and Methods

The materials used for this study included ASTM C595 Type IL cement (ASTM C595), slag, silica fume, and a fine masonry sand. Two different mix designs were selected to ensure there were different flow properties between the mixes without much change in tensile performance. Table 1 shows the mix proportions used for the two mixes. They are labeled with their target compressive strength, as determined by previous trial mixes. All mixes used high-strength steel fibers with a 0.5 in. (13 mm) length and 0.008 in. (0.2 mm) diameter at a 2.0% volume percentage.

The test method used to measure interlayer tensile strength was based off of ASTM C1583 (ASTM C1583). Specimens were cast by placing a 2.5 in. (64 mm) thick layer of concrete initially and then waiting a prescribed amount of time until adding an additional 1.5 in. (38 mm) of concrete on top. Specimens were not covered or troweled between placement of the first and second layer. The concrete for the second layer was dyed red to help visually define the interface between the layers. The molds were 4 × 4 × 14 in. (100 × 100 × 360 mm) rectangular steel prism molds. Three

Table 1. Mix design proportions

Material	15-18 ksi lb/yd ³ *	18-21 ksi lb/yd ³ *
Sand	1815	1588
IL Cement	1404	1597
Slag	272	309
Silica Fume	136	155
Water	362	335
HRWR admixture	16.4	30.9
HRWR + workability retaining admixture	16.4	30.9
Surface-enhancing admixture	3.4	5.2

*1 lb/yd³ = 0.5933 kg/m³

cores were drilled 2.5 in. (38 mm) deep into each prism, resulting in three test specimens that met the spacing requirements in ASTM C1583. Figure 1 shows a diagram of a prism with the three cores.

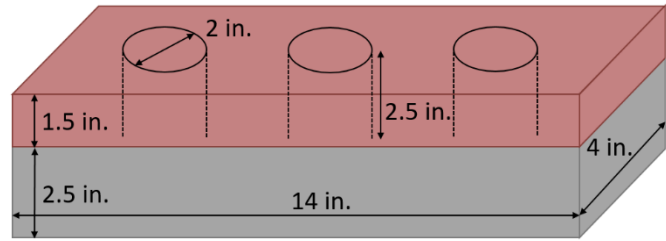


Figure 1. Dimensioned diagram of test specimens

Testing was performed to determine how different UHPC fresh properties, times between layers, and consolidation methods affected the bond strength between layers. For each mix design and time interval used, three different consolidation methods were applied. The control placement method used no consolidation. The second consolidation method was external vibration in which specimens were cast on a vibrating table that was turned on for 10 seconds after the second layer was placed. The final consolidation method was rodding. This method used a tamping rod pushed vertically through both layers of concrete after the second layer had been placed. Each rectangular prism was rodded six times in equidistant locations on the surface. All specimens were finished with a trowel after consolidation and covered to prevent evaporation.

The flow diameter of each concrete batch was tested in accordance with ASTM C1856 at the time of placement (ASTM C1856). In addition, at the time of placement of the top layers of concrete, the stiffness of the bottom layer was measured. The stiffness of the bottom layer was tested with a Vicat needle with a diameter of 0.79 in. (20 mm) and a length of 2.04 in. (51.8 mm). The typical metal Vicat shaft was replaced with a lightweight plastic one with a 0.40 in. (10.3 mm) diameter. A portable stand was made using a plastic disk base with a hole through the middle and a vertical glass tube. The base had a diameter slightly less than 4 in. (102 mm), and the tube had an inner diameter of 0.49 in. (12.5 mm). After placing the stand and needle on the concrete's surface, weights were slowly added to the Vicat needle shaft until it pierced through the elephant skin. The weight of the needle plus any added weights was recorded. The combined weight of the needle and the attached shaft was 0.99 oz (28 g). The added weights were metal with holes through the center so they could be balanced on the metal holder atop the needle shaft. Combination of large weights weighing 1.6 oz (45 g) and smaller weights weighing 0.32 oz (9 g) each were used to get a more precise measure of the stiffness. While this was not a standard method for measuring surface stiffness, it gave a quantitative value to compare the relative stiffness of the elephant skin when the second layer of concrete was placed.

The first specimens had both layers made from the same mix, with the concrete continuously mixing between placements. This resulted in workability loss for the top layers of concrete, especially for longer intervals. Subsequent specimens were made by using a separate mixer for each layer and waiting a prescribed amount of time before starting the second batch, allowing it to be placed directly from the mixer. The mix designs were identical, but the mixer and batch size were different, which may have affected the resulting properties.

Specimens were demolded after one day and cured according to ASTM C31 (ASTM C31). Specimens were briefly removed from the curing environment to be cored with a 2.5 inch (64 mm) outer diameter bit, resulting in a 2-inch core (51 mm). At roughly 26 days, specimens were

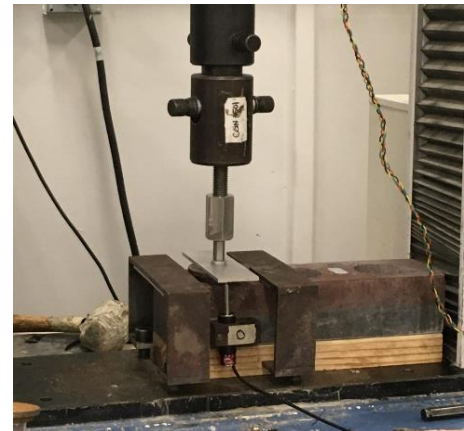


Figure 2. Pull-off testing setup

removed from the curing environment so they could dry prior to the attachment of aluminum pull-off discs on each core surface. Pull-off discs were attached with Sikadur 31 epoxy and cured for two days.

At 28 days, specimens were tested using a pull-off test based on ASTM C1583 (ASTM C1583) using a 30 kip (133 kN) capacity universal testing machine. The setup is shown in Figure 2. The specimen was stabilized using metal brackets bolted to the testing surface. An attachment with a two-way pin was screwed into the aluminum disk epoxied to the core top and attached to the machine. LVDTs were used to determine displacement between the bottom of the core and the top of the aluminum disk.

3. Results

Table 2 shows the mixes from which prisms were made using the various consolidation methods. It shows the mass required for the Vicat needle to puncture through the Layer 1 elephant skin in the “Layer 1 stiffness” column.

The location of each break was recorded as being either in the bottom layer, the interface between the layers, the top layer, or near the epoxy attaching the metal pull-off disk to the top of the core. Figure 3 shows broken cores after testing.

From left to right, the specimen had failures at the interface, epoxy, and bottom of the core. No breaks occurred in the top layer of concrete for any test. Most breaks, including those that occurred in the bottom layer of concrete, were brittle and therefore did not produce useful stress vs. strain data. Specimens that broke within the bottom layer of concrete experienced a decrease in stress of over 50% immediately after cracking. Specimens breaking in the epoxy or at the layer interface showed an immediate drop to zero strength after cracking. Based on these results, the predominant data used to compare the specimen results were the peak stress and location of failure.

The cracking stress for the cores was highly varied. Interface strengths ranged from 0–800 psi (0–5.50 MPa), and the strength of failures at the core bottom ranged from 250–1125 psi (1.72–7.76 MPa) The strength of the failures through the epoxy ranged from 275-910 psi (1.90-6.27 MPa), but this only gave a minimum strength which both the interface and concrete layers exceeded. With this in mind, Figure 4 was created to show the maximum strength of the specimens that failed at the interface or core bottom. The horizontal line in the center of each box indicates

Table 2. Mixes used and fresh properties

Mix Design (ksi)	Time Interval (min)	Batches for layers	Layer 1 stiffness (grams)	Layer 2 flow (inches)
18	10	same	28	7.9
15	10	different	37	7.1
18	10	different	37	9.5
18	20	same	82	6.6
18	20	different	41.5	9.4
15	35	different	253+	5.5
18	35	different	163	9.8

+ Denotes weight apparatus was at maximum capacity.

1 ksi = 6.895 MPa

1 g = 0.0353 oz



Figure 3. Concrete cores after testing

the median while the “X” represents the mean. The box shows the interquartile range, calculated using the inclusive median. As Figure 4 shows, the specimens with layers placed at a 35-minute interval had the weakest average and median bond strengths. This was especially true for the specimens consolidated with rodding or external vibration. The control specimens had similarly low average breaks for all time intervals. The rodded specimens had higher strengths on average than the vibrated specimens.

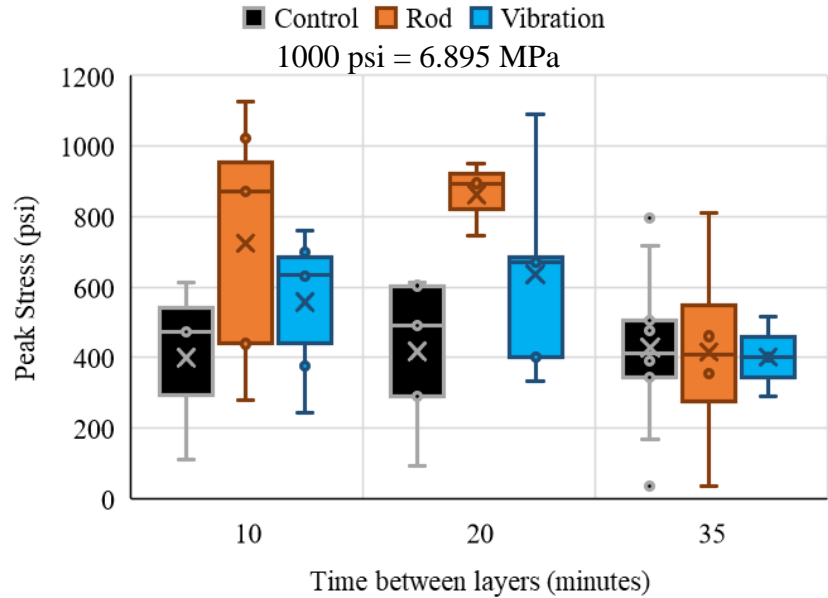


Figure 4. Box and whisker plot of failure strength vs. time

Due to the brittle nature of interface failures, the percentage of failures that occurred at the layer interface was examined and is shown in Table 3. There are also overall statistics presented for each time interval and consolidation method. This table demonstrates that at any time interval, interface failures were more common for control specimens than they were for the rodded or vibrated specimens. In fact, none of the specimens with either a 10- or 20-minute interval between layers failed at the layer interface if they had been rodded or vibrated. This table also shows a clear change in the control specimens as the time interval increased. Even though the mean and median breaking strengths for control specimens were relatively unaffected by time interval, Table 3 illustrates how the location of those failures was greatly affected by the time interval.

Table 3. Percentage of interface failures

Time interval	Control	Rod	Vibration	Overall
10 minutes	33%	0%	0%	10%
20 minutes	60%	0%	0%	23%
35 minutes	100%	25%	100%	81%
Overall	76%	7%	23%	38%

4. Discussion

Ideally, the strength of failures at the core bottom should reflect those of a solid pour; however, direct tension testing of this same mix using the FHWA method (Graybeal and Baby) produced more consistent results with a much greater average peak stress of 1100 psi (7.58MPa). There are multiple potential reasons for lower and more variable pull-off strengths. One is preferential fiber orientation, which is in the direction of testing for direct tension specimens but perpendicular for pull-off specimens. In addition, the fibers along the edge of the pull-off specimen had been cut in the coring process, reducing their effective length. Finally, the FHWA direct tension test is designed to reduce stress concentrations and eccentric loads, but the pull-off test produces very high stress concentrations at the base of the core.

To better understand the mechanisms affecting break strength and location, selected specimens were scanned using x-ray computed tomography (CT). The 3-D images are shown with only the

fibers visible to see through a larger portion of the specimen. Most specimens scanned were cores that had already been tested, but larger sections of the prisms were used for rodded specimens to see how individual rodding motions would affect different areas of the panels. Figure 5 shows a core that failed at its base during testing and was later scanned. This image clearly shows the interface between top and bottom layers that few fibers cross. It also shows few vertical fibers overall, which helps explain the low post-cracking strength of all failures, including ones at the core base.

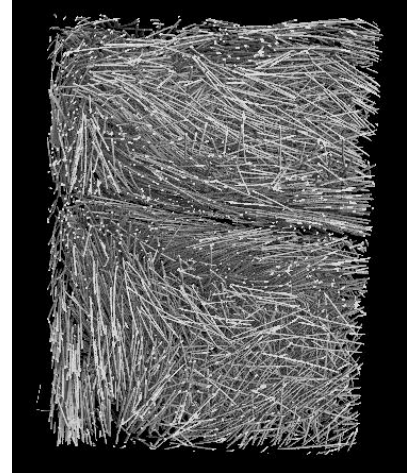


Figure 5. CT scan of control core

For specimens with layers 10 and 20 minutes apart, the rodded specimens had the highest average strength. For 35-minute specimens, average strengths were roughly equal, but the rodded specimens had a lower percentage of breaks occurring at the interface. It is theorized that this is due to the rodding motion re-orienting fibers in a vertical direction and forcing the layers to intermix. Figure 6 shows a CT scan of a slice of rodded specimen. It can be seen in the circled sections that the fibers are oriented much more vertically in the location of rodding than in the surrounding sections.

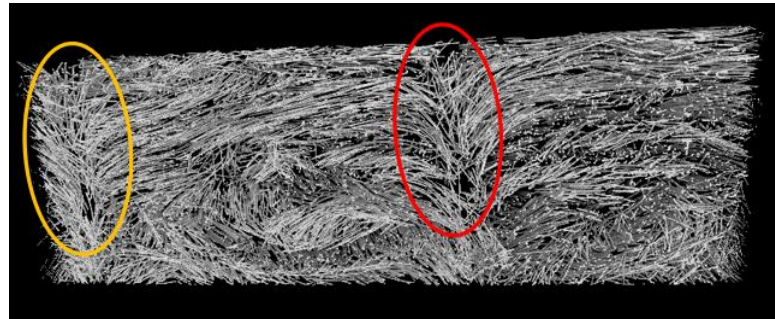


Figure 6. CT scan of rodded specimen

This explains why rodded specimens had higher strengths when tension was applied vertically to cores. Figure 6 also shows that the specimen region affected by rodding was small. These specimens were rodded once for every 9 in.² (58 cm²) of interface area, which may be difficult to achieve for a large-scale member. Figure 7 shows a cut surface of a specimen after testing where the rodding location can be clearly seen by the color difference in layers. Like Figure 6, Figure 7 shows that the region influenced by rodding is small. It also shows that rodding tended to push the entire interface downward rather than pushing fibers through the interface. Other than a small region at the bottom of the rodding location, there is not much intermixing of the layers. However, this would still improve the tensile strength by angling the interface with respect to the load and increasing the interface area.



Figure 7. Rodded interface of cut specimen

An important consideration for rodded specimens is the introduction of large voids. Figure 8 shows a 2D view of the same rodded specimen shown in Figure 6, with the red circle locations aligned. Figure 8 displays both concrete and fibers in the image, revealing a large air void at the location of rodding. Rodding voids were seen in multiple locations for the specimen rodded at 35 minutes, when the bottom layer had stiffened significantly. This specimen maxed out the Vicat needle weight without its elephant skin breaking, making it by far the stiffest mix at the time the

second layer was placed. Specimens rodded after shorter wait periods did not show these voids, so it is reasonable to assume the introduction of air voids due to rodding would be uncommon for mixes with good workability retention or shorter intervals between placements.

It should be noted that the correlation between the time the placed concrete was resting and its resistance to the Vicat needle had an R^2 value of 0.819. Increased time after placement would increase both desiccation of the elephant skin and curing of the concrete beneath it. However, this research tested only two different mix designs, and different UHPC mixes may have different consistencies at later times. This is an advantage of using a surface stiffness test such as the Vicat needle – the results are based on the particular mix as well as any environmental factors such as temperature and humidity that could affect stiffness. While a time limit between placements would not require testing of the specimen surface, it could be difficult to determine, as one batch placement can take 15 minutes by itself to complete. A similar problem arises if a surface stiffness test is introduced, as a large concrete member could have different concrete stiffness measurements in different locations. It is clear that a time difference of over 30 minutes between placements is detrimental to the integrity of the bond between those placements, especially if no consolidation method is used. For the needle test, a stiffness limit of 7 oz (200 g) or less of needle weight could be required to allow a second concrete placement on a specimen. For needle weights between 3.5-7 oz (100-200 g), a consolidation method could be required after the second placement has been made.

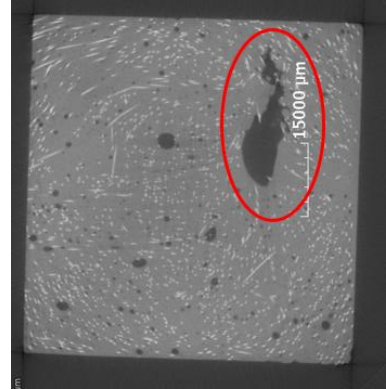


Figure 8. Air void in rodded specimen

5. Conclusions

The following conclusions were drawn from this research.

1. Concrete placed in multiple batches should be rodded or otherwise mechanically mixed at the interface between the two batches to increase bond strength and to vary fiber orientation throughout the specimen. Rodding may introduce air voids into stiffened concrete.
2. Concrete placed in multiple layers will ideally have less than a 30 minute time interval between placements to improve bond strength and increase the strength in the interface.
3. A needle test used to measure surface stiffness correlated well to the amount of time between placements and helped to quantitatively indicate elephant skin stiffness. A similar method could be used in the field to specify limits and determine when consolidation is needed.
4. The flow of the second layer of concrete had little impact on bond strength when compared to the stiffness of the lower layer's elephant skin.

Based on the results from this research, the researchers recommend that specification agencies limit either the time between layers or the stiffness of the bottom layer at the time of a second placement.

6. Acknowledgements

The authors would like to thank the Florida Department of Transportation for funding this work under contract number BDV31 977-105. The opinions, findings, and conclusions expressed in this

publication are those of the authors and not necessarily those of the Florida Department of Transportation. The authors thank Argos USA, LLC; Sika USA, and Edgar Minerals for material donations. Special thanks to Ashish Patel, Daniel Alabi, Leonard Iacopelli, Maxwell Armstrong, Robbie Posada, and Connor Cronin for help with mixing and testing.

7. References

- Standard Practice for Making and Curing Concrete Test Specimens in the Field, ASTM C31, ASTM International, West Conshohocken, PA, 2019.
- Standard Specification for Blended Hydraulic Cements, ASTM C595, ASTM International, West Conshohocken, PA, 2019.
- Standard Test Method for Tensile Strength of Concrete Surfaces and the Bond Strength or Tensile Strength of Concrete Repair and Overlay Materials by Direct Tension (Pull-off Method), ASTM C1583, ASTM International, West Conshohocken, PA, 2020.
- Standard Practice for Fabricating and Testing Specimens of Ultra-High Performance Concrete, ASTM C1856, ASTM International, West Conshohocken, PA, 2017.
- Binard, J. “UHPC: A Game-Changing Material for PCI Bridge Producers.” *PCI Journal*, vol. 62, no. 2, 2017, pp. 34–46.
- Concrete Materials and Methods of Concrete Construction, CSA A23.1:19, Canadian Standards Association, 2019, pp. 379–409.
- Ganesh, P., and A. Ramachandra Murthy. “Simulation of Surface Preparations to Predict the Bond Behaviour between Normal Strength Concrete and Ultra-High Performance Concrete.” *Construction and Building Materials*, vol. 250, 2020,
- Graybeal, Ben. “Design and Construction of Field-Cast UHPC Connections”. 2014.
- Graybeal, Benjamin, and Florent Baby. “Development of Direct Tension Test Method for Ultra-High-Performance Fiber-Reinforced Concrete.” *ACI Materials Journal*, vol. 110, no. 2, 2013, pp. 177–86.
- Miguel A. Carbonell Muñoz, et al. “Bond Performance between Ultrahigh-Performance Concrete and Normal-Strength Concrete.” *Journal of Materials in Civil Engineering*, vol. 26, no. 8, Aug. 2014, p. 4014031.
- Yalçinkaya, Çağlar, and Oğuzhan Çopuroğlu. “Elephant Skin Formation on UHPC Surface: Effects of Climatic Condition and Blast Furnace Slag Content.” *Construction and Building Materials*, vol. 268, 2021.